

# Enhanced Color Purity of Alternating Current-Driven Micro-Cavity Organic Light Emitting Diode

Duck-Kyu Lim<sup>1</sup>, Byeonggon Kim<sup>1</sup>, and Hak-Rin Kim<sup>1,\*</sup>

<sup>1</sup>School of Electronics Engineering, Kyungpook National University, Daegu 41566, Korea

Keywords: Micro-cavity effect, Polyfluorene, Color purity, Solution process, Purcell effect.

## ABSTRACT

We introduced the micro-cavity effect on Alternating Current-Driven Polymer Light Emitting Diodes and investigated the color purity enhancement effect depending on the organic layer thickness condition. We have analyzed the electric field inside the device by the finite-difference time-domain method and fabricated the designed optimal devices.

## 1 INTRODUCTION

Organic light emitting diodes (OLEDs) have been applied to television and mobile phones as next generation displays replacing liquid crystal displays (LCDs). Since OLEDs does not need back light unit, it can have a free form factor. Also, it has many advantages such as fast response time and infinite contrast ratio. After the light emission has been confirmed in polymers, many polymer electro-luminescence (EL) devices have been studied. Unlike single molecular materials using the evaporation process, the polymers with side chain enable the solution process that has many advantages such as fast process time, and large area fabrication. However, when a polymer is used for EL devices, there are still some problems to be solved like low color purity. In particular, these drawbacks are noticeable in short wavelength light emitting materials requiring a larger bandgap. Polyfluorene (PFO), shown in Fig. 1 (a), is one of the blue emitting polymers and currently being investigated for use in light emitting devices or field effect transistors. In PFO, photo-oxidation and thermal-oxidation effects lead to fluorenone defects yielding fluorenone moieties combined with the PFO backbone, shown in Fig. 1 (b) [1]. This defects are responsible for the 530nm region emission.

To produce a simple structure device using a solution process, an alternating current (AC)-driven OLED was introduced. The common direct current (DC)-driven OLED requires holes and electrons to be injected at anode and cathode respectively, which requires each injection and transport layer. For that reason, the layer structure is complicated and the process time is long. The AC-driven OLED is composed of only two layers, an insulating layer and emitting layer mixed with carbon nanotube (CNT) [2], [3]. In this structure, electrons and holes are injected from a single electrode. The CNT mixed in the light emitting layer sufficiently lowers the energy barrier between the electrode and the light emitting layer. When negative voltage is applied on anode, holes are injected and

accumulated at the interface between the light emitting layer and the insulating layer through the CNT. When positive voltage is applied on anode, electrons are injected through the CNT and recombination occurs resulting in light emission.

The micro-cavity effect was applied to DC-driven OLEDs fabricated by the deposition process to increase the color purity [4], [5]. Distributed Bragg reflector or thin metal was used for the semitransparent layer [6], [7]. Since the DC-driven OLEDs were manufactured in many layers, it takes a lot of time. Thus, we introduced the micro-cavity effect on AC-driven OLEDs structure, which can be manufactured in a simple layer structure using a solution process, and investigated the color purity improvement effect depending on the dielectric layer thickness condition under the emissive layer.

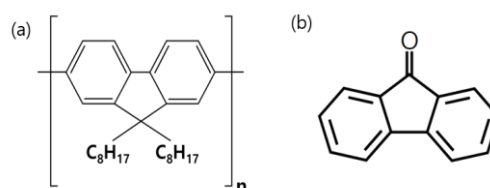


**Fig. 1 (a) The chemical structure of the poly(9,9-dioctylfluorenyl-2,7-diyl). (b) The chemical structure of fluorenone.**

## 2 EXPERIMENT

Fig. 2 shows newly proposed AC-driven OLEDs structure and operating mechanism. For the designed thickness, we controlled the weight percent of the polymer. Indium tin oxide (ITO) was deposited to 150nm on 0.7T glass. Then semitransparent thin Aluminum (Al) was deposited at a high vacuum of  $2 \times 10^{-6}$  torr. Ultraviolet ozone was treated for 20 minutes to increase the surface energy. This treatment also has a cleaning effect. Polyimide (PI) was spin coated at 3000 rpm and pre-baked at 65°C and post-baked at 230°C. PFO was dissolved in toluene at 0.8 weight percent for the designed thickness. When the PFO is completely dissolved, CNTs (SA230, Nano-solution Ltd.) were mixed with the solution. This solution was bath-sonicated (NXPC-2010, Kodo Technical Research Co., Ltd) for 1 hours. The CNTs capped by PFOs were well dispersed and did not aggregate because the PFO side chain has a good solubility in toluene. Then, the PFO solution was spin-coated at 2000 rpm and pre-baked at 70°C and

post-bake 180°C. The Al Cathode was deposited through a thermal evaporation process at a high vacuum of 2 x 10<sup>-6</sup> torr.

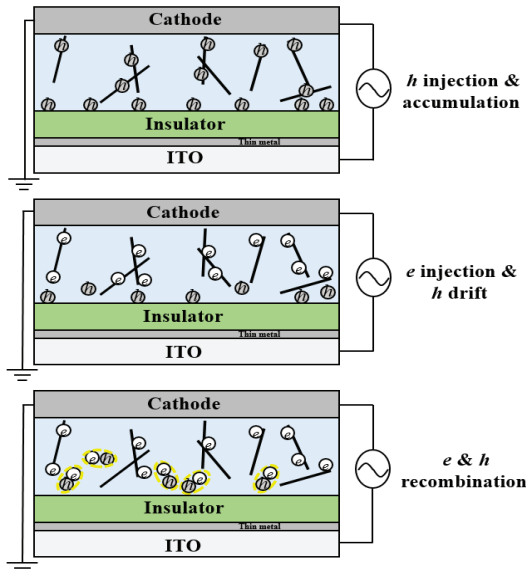


**Fig. 2 Schematic diagram of the operating mechanism for the AC-Driven OLED with CNT.**

The EL spectrum of fabricated OLEDs was analyzed by using the spectroscopy equipment (fluoromax-4, Horiba Ltd.). Time-resolved photoluminescence (TRPL) measurement was conducted using a confocal microscope system (MicroTime-200, Picoquant Ltd.) with a 10× objective. The lifetime properties were analyzed through the TRPL measurement result. A single-mode pulsed diode laser, which has the wavelength of 375 nm and pulse width of 30 ps, was used as an excitation source. A dichroic mirror (Z375RDC, AHF), a longpass filter (HQ405lp, AHF), a band-pass filter (430 or 500 nm), and an avalanche photodiode detector (PDM series, MPD) was used to collect emission photons from the samples. Exponential fitting for the obtained PL decays was accomplished using the Symphotime-64 software.

### 3 OPTICAL ANALYSIS

Reflection of the PFO-Al interface and reflection of the thin Al-PI interface induces a micro-cavity effect. When the intensity of the light generated in the emitting layer, which is not in the cavity mode, is  $I_0$ , the intensity of light generated in the cavity mode is expressed as  $G(\lambda) \cdot I_0$ .  $G(\lambda)$  is the cavity enhancement factor and is expressed by the following equation :

$$G(\lambda) = f_{\text{fabry-perot}}(\lambda) \times f_{\text{interference}}(\lambda). \quad (1)$$

Fabry-perot interferometer equation  $f_{\text{fabry-perot}}(\lambda)$  made from two parallel reflecting mirrors is given by :

$$f_{\text{fabry-perot}} = \frac{T_{\text{Thin Al}}}{(1 - \sqrt{R_{\text{Al}} R_{\text{Thin Al}}})^2 + 4\sqrt{R_{\text{Al}} R_{\text{Thin Al}}} \sin^2\left(\frac{\Delta\phi}{2}\right)}, \quad (2)$$

$$\Delta\phi = -\phi_{\text{Al}} - \phi_{\text{Thin Al}} + \sum \frac{4\pi n T \cos\theta}{\lambda}, \quad (3)$$

in which reflectivity and transmittance can be calculated from the Fresnel equation using refractive index and absorption coefficient of each materials.  $\Delta\phi$  is the round-trip phase and  $\cos(\theta)$  is the incident angle. When the incident angle increases, the resonance wavelength shifts to a short wavelength. As light travels through the material, the optical path length is increased by the refractive index ( $n$ ). The resonance wavelength is determined according to the thickness ( $T$ ) of the organic layer between the two metals. In addition, the phase shifts when reflected from the metal must be considered. Two beam interference equation  $f_{\text{interference}}(\lambda)$  is given by :

$$f_{\text{interference}} = 1 + R_{\text{Al}} + 2\sqrt{R_{\text{Al}}} \cos\left(-\phi_{\text{Al}} + \frac{4\pi n L \cos\theta}{\lambda}\right), \quad (4)$$

in which the distance ( $L$ ) between the light emitting layer and the thick Al surface should be designed so that the light going up and the light reflected from the bottom become the constructive interference.

Based on the equation described above, the internal electric field of the metal layer between two metals should be considered [8] - [11]. We simulated the internal electric field by using the finite-difference time-domain (FDTD) method. This method solves Maxwell's equations on a discrete spatial and temporal grid. The refractive index of a general organic material has a value of 1.6 to 1.8. Fig. 3 shows the refractive index of PI and PFO.

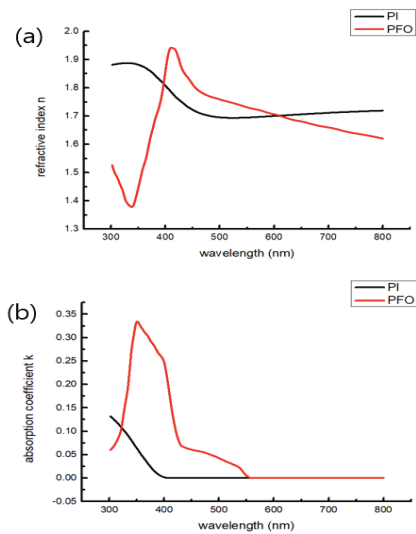


**Fig. 3 (a) Refractive index of organic materials. (b) Absorption coefficient of organic materials.**

The PFO is light emitting material with a large absorption coefficient ( $k$ ) in the 380 nm band and the PI is a transparent material because of its low absorption coefficient in the visible light range. The refractive index of thin Al was measured using an ellipsometry instrument and other layers were applied with a database of setfos simulator. The electric field of the mesh grid inside the cavity structure can be calculated by injecting a plane wave from the thin Al side.

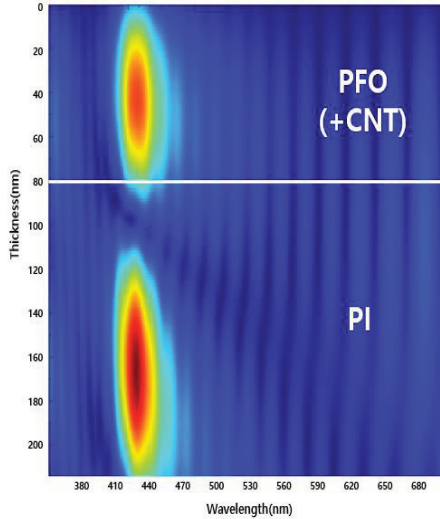


**Fig. 4 Internal electric field in cavity structure by using FDTD method.**

Since PI was thinned even at 50 nm level, 1st mode cavity structure was impossible to drive at high voltage. Therefore, for the thickness of PI that can be driven, organic layers were designed with a 2nd mode cavity structure in which two antinodes exist. As shown in Fig. 4, the resonance frequency was set to 430 nm, which is the main peak of PFO. As the intensity of the electric field changes depending on the position inside the device, dipole position is important factor.

If the dipole is positioned inside the resonator, a Purcell effect occurs in which the spontaneous emission is modified [12], [13]. According to Fermi's golden rule, the transition rate is proportional to the density of state. In cavity structure, the density of state increases resulting in the increase of transition rate. If the radiative decay rate in the infinite medium is  $\Gamma_0$ , the radiative decay rate in the cavity  $\Gamma_r^*$  is modified to be

$$\Gamma_r^* = F \times \Gamma_0, \quad (5)$$

where  $F$  is the so-called Purcell factor. Generally, the non-radiative decay rate  $\Gamma_{nr}$  is a constant, the internal quantum efficiency  $\eta_{int}$  becomes

$$\eta_{int} = \frac{\Gamma_r^*}{\Gamma_r^* + \Gamma_{nr}}. \quad (6)$$

Since the decay rate and the lifetime have an inverse relationship, the lifetime in the resonator structure is shortened.

#### 4 RESULT AND DISCUSSION

Fig. 5 shows the EL spectrum of AC-driven OLEDs under the condition of 30 V, 500 kHz. The reference device structure without semitransparent thin Al is GLASS / ITO / PI / PFO / Al, and the cavity device structure is GLASS / ITO / thin Al / PI / PFO / Al. Both reference and cavity structure devices were turned on at 15 V. Owing to the sufficient thickness of PI, devices can be driven to 60 V high voltage. Because the device is operated by AC power,

there is a frequency dependency. As the operating frequency increased to 500 kHz, the EL intensity of the device increased. However, above 500 kHz, the EL intensity decreased. When the operating frequency is too low, injected holes or electrons are quenched by trap or non-radiative losses, before the polarity of the voltage changes. Therefore, the exciton formation is insufficient and the luminance decreases. As the operating frequency increases, the quenching process decreases and the EL intensity increases. Above 500 kHz, the luminance decreased, because the carrier mobility was too low to respond to the operating frequency. In other words, the excitons were not sufficiently generated.

The spectrum shows that the resonance frequency was set to 430 nm. Thus, it was confirmed that the fluorenone defect emission of green band is effectively suppressed resulting in the color change from sky blue to blue. Also, in CIE 1931 color space, the coordinates moved from (0.25, 0.35) to (0.24, 0.29) as shown in Fig. 6. That is, the destructive interference occurred in 530 nm wavelength emission band. The inherent problem of the blue emitting polymers was improved by introducing optimal device designs.

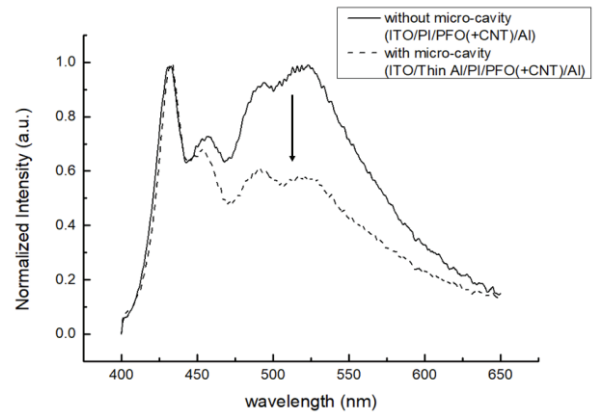


**Fig. 5 EL spectrum in AC OLED driven at 500 kHz.**

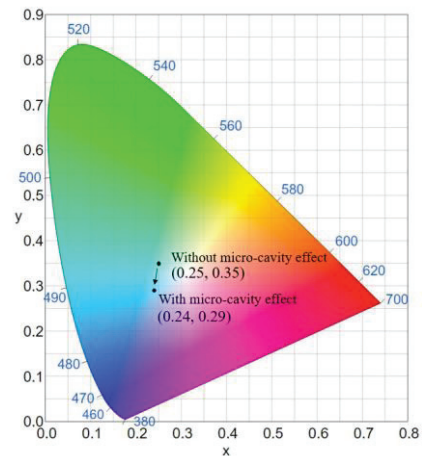


**Fig. 6 CIE 1931 color space value of AC-driven OLEDs showing enhanced color purity.**

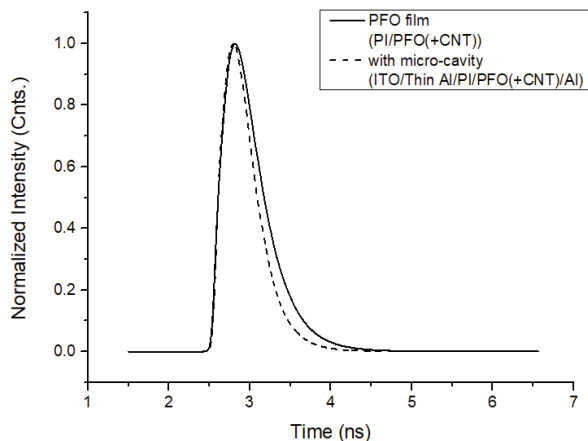


**Fig. 7 Decay curves of AC-driven OLEDs with micro-cavity effect.**

**Table 1. The parameters of fitted curve intensity**

	A1	$\tau_1(ns)$	A2	$\tau_2(ns)$	$\tau_{average}(ns)$
PFO film	23	0.28	0.0157	3.6	0.3099
Micro-cavity device	23	0.2245	0.0169	2.4	0.242

The lifetime of PFO film and micro-cavity structure was measured by TRPL measurement using a 430 nm wavelength filter. After being excited using a 375 nm wavelength beam, residual photons are accumulated to create a decay curve. The average lifetime of PFO film is 0.3 ns. Fig. 7 shows that the fluorescence lifetime is shorter in the micro-cavity structure than in the PFO film. This means that the Purcell effect appears on the dipole between two metallic cavity. Therefore, this shorten lifetime result is evidence of increased radiative decay rate.

## 5 CONCLUSIONS

We fabricated AC-driven micro-cavity OLEDs that can emit light with a simple structure different from DC-driven OLEDs. The optical analysis was performed using the FDTD method and the optimum layer thickness was designed with the resonance frequency set to PFO's main peak. By using the micro-cavity effect, the green region emission from the fluorenone defect was effectively suppressed. In addition, the PFO lifetime was shorten by resonance structure which means the increased transition rate. Therefore, it is possible to overcome the inherent limitations of polymers by adding semitransparent thin Al to the AC-driven OLEDs.

## ACKNOWLEDGMENT

This work was supported by the National Research Foundation of Korea (NRF) grant funded by the Korea government (MSIT) (No 2019R1A2C1005531).

## REFERENCES

[1] S. S. Xiao, G. C. Bazan, P. K. Iyer, A. J. Heeger, X.

Gong, and D. Moses, "Stabilized Blue Emission from Polyfluorene-Based Light-Emitting Diodes: Elimination of Fluorenone Defects," *Adv. Funct. Mater.*, vol. 13, no. 4, pp. 325-330 (2003).

- [2] J. Sung, Y. S. Choi, S. J. Kang, S. H. Cho, T. W. Lee, and C. Park, "AC field-induced polymer electroluminescence with single wall carbon nanotubes," *Nano Lett.*, vol. 11, no. 3, pp. 966-972 (2011).
- [3] S.-Y. Jeon and S. Yu, "AC-driven organic light emission devices with carbon nanotubes," *J. Korean Phys. Soc.*, vol. 70, no. 4, pp. 442-445 (2017).
- [4] M. J. Park et al., "Device performances of third order micro-cavity green top-emitting organic light emitting diodes," *Org. Electron. physics, Mater. Appl.*, vol. 26, pp. 458-463 (2015).
- [5] R. H. Jordan, L. J. Rothberg, A. Dodabalapur, and R. E. Slusher, "Efficiency enhancement of microcavity organic light emitting diodes," *Appl. Phys. Lett.*, vol. 69, no. 14, pp. 1997-1999 (1996).
- [6] K. Neyts, P. De Visschere, D. K. Fork, and G. B. Anderson, "Semitransparent metal or distributed Bragg reflector for wide-viewing-angle organic light-emitting-diode microcavities," *J. Opt. Soc. Am. B*, vol. 17, no. 1, pp. 114-119 (2007).
- [7] R. Pode et al., "Efficient micro-cavity top emission OLED with optimized Mg:Ag ratio cathode," *Opt. Express*, vol. 25, no. 24, p. 29906 (2017).
- [8] J. Chan et al., "Cavity design and optimization for organic microcavity OLEDs," *Proc. SPIE*, vol. 6038, pp. 464-472 (2006).
- [9] C. L. Lin, T. Y. Cho, C. H. Chang, and C. C. Wu, "Enhancing light outcoupling of organic light-emitting devices by locating emitters around the second antinode of the reflective metal electrode," *Appl. Phys. Lett.*, vol. 88, no. 8, pp. 1-4 (2006).
- [10] T. Y. Cho, C. L. Lin, and C. C. Wu, "Microcavity two-unit tandem organic light-emitting devices having a high efficiency," *Appl. Phys. Lett.*, vol. 88, no. 11, pp. 1-4 (2006).
- [11] M. Furno, R. Meerheim, S. Hofmann, B. Lüsse, and K. Leo, "Efficiency and rate of spontaneous emission in organic electroluminescent devices," *Phys. Rev. B - Condens. Matter Mater. Phys.*, vol. 85, no. 11, pp. 1-21 (2012).
- [12] X. W. Chen, W. C. H. Choy, C. J. Liang, P. K. A. Wai, and S. He, "Modifications of the exciton lifetime and internal quantum efficiency for organic light-emitting devices with a weak/strong microcavity," *Appl. Phys. Lett.*, vol. 91, no. 22, p. 221112 (2007).
- [13] X. W. Chen, W. C. H. Choy, S. He, and P. C. Chui, "Comprehensive analysis and optimal design of top-emitting organic light-emitting devices," *J. Appl. Phys.*, vol. 101, no. 11, p. 113107 (2007).